

# Thermoelectric studies of $K_xFe_{2-y}Se_2$ indicating a weakly correlated superconductor

Kefeng Wang (王克锋), Hechang Lei (雷和畅), and C. Petrovic

*Condensed Matter Physics and Materials Science Department, Brookhaven National Laboratory, Upton, New York 11973, USA*

(Received 11 February 2011; revised manuscript received 15 March 2011; published 4 May 2011)

We report thermal transport properties of a  $K_xFe_{2-y}Se_2$  superconducting single crystal. A peak anomaly in the thermal conductivity is observed at nearly  $T_c/2$ , attributed to phonons. The thermoelectric power above  $T_c$  exhibits nearly linear behavior and could be described well by the carrier diffusion mechanism in a wide temperature range. The zero-temperature extrapolated thermoelectric power is smaller than the value in typical strongly correlated superconductors, implying a large normalized Fermi temperature. These findings indicate that  $K_xFe_{2-y}Se_2$  is a weakly or intermediately correlated superconductor.

DOI: [10.1103/PhysRevB.83.174503](https://doi.org/10.1103/PhysRevB.83.174503)

PACS number(s): 74.25.fc, 74.25.fg, 74.20.Mn, 74.70.Xa

## I. INTRODUCTION

The discovery of a superconducting transition temperature up to  $T_c = 26$  K in  $LaFeAsO_{1-x}F_x$  (1111 type) with  $x \sim 0.11$  (Ref. 1) generated intense activity.<sup>2,3</sup> Soon it was discovered that the superconducting transition temperature can be pushed to higher values by substituting La ions with heavier rare earths,<sup>4-6</sup> and the highest  $T_c \sim 55$  K was achieved in  $SmO_{1-x}F_xFeAs$  (Ref. 7) and  $\sim 56.3$  K in  $Gd_{1-x}Th_xFeAsO$ .<sup>8</sup> Superconductivity was also discovered in doped  $AFe_2As_2$  compounds (122 type,  $A = Ba, Sr, Ca$ ) with  $ThCr_2Si_2$  structure,<sup>9-11</sup> which contain a double FeAs plane,  $Fe_2As$ -type  $AFeAs$  (111 type,  $A = Li$  or  $Na$ ),<sup>12,13</sup> as well as anti-PbO-type  $Fe(Se,Te)$  (11 type).<sup>14,15</sup> The pairing mechanism and order parameter symmetry in new superconductors became important issues.  $s_{\pm}$  superconductivity was proposed, in which the sign of the order parameter is switched between the two sets of Fermi surfaces.<sup>16,17</sup> A multiband electronic structure and interpocket hopping or Fermi surface nesting seemed to be common ingredients in all iron-based superconductors.<sup>16-18</sup> However, after more iron-based superconductors were observed, consensus seems further away.<sup>19-22</sup>

Recently, a new series of iron-based superconductors  $A_xFe_2Se_2$  ( $A = K, Rb, Cs, Tl$ ) has been discovered with relatively high  $T_c \sim 30$  K.<sup>23-27</sup> These compounds are purely electron doped and it is found that the superconductivity might occur in the proximity of a Mott insulator.<sup>25</sup> The low-energy band structure and Fermi surface of  $K_xFe_{2-y}Se_2$  may be different from those of other iron-based superconductors. Only electron pockets were observed in angle-resolved photoemission experiments without a hole Fermi surface near the zone center.<sup>28-30</sup> This indicates that the sign change and  $s_{\pm}$ -wave pairing are not fundamental properties of iron-based superconductors.

Thermal transport measurement is an effective method to probe the superconducting state and transport properties in the normal state in high- $T_c$  cuprates and iron-based superconductors.<sup>31-37</sup> In  $SmFeAsO_{0.85}$ , the magnitude of the thermoelectric power (TEP) develops a broad peak above  $T_c$  coupled with a metallic resistivity behavior. This is attributed to resonant phonon scattering between electron and hole pockets indicating a significant Fermi surface nesting in this system.<sup>32</sup> The TEP in doped  $BaFe_2As_2$  also pointed to a significant modification of the Fermi surface at small electron doping, stabilizing low-temperature superconductivity.<sup>33</sup> In

the  $Fe_{1+y}Te_{1-x}Se_x$  system, the TEP and Nernst coefficients provide evidence of a low-density and strongly correlated superconductor.<sup>34</sup> Finally, the thermal conductivity at very low temperature provides insight into the superconducting gap structure.<sup>19,37</sup>

Here we report temperature- and magnetic-field-dependent thermal transport of a  $K_xFe_{2-y}Se_2$  single crystal. A peak in the thermal conductivity [ $\kappa(T)$ ] is observed at about  $\frac{T_c}{2}$ , which is attributed to phonons. The thermoelectric power above  $T_c$  exhibits nearly linear behavior and could be described well by the carrier diffusion mechanism in a wide temperature range. The Fermi temperature  $T_F$  deduced from these measurements yields a smaller  $T_c/T_F$  than the value in the  $Fe_{1+y}Te_{1-x}Se_x$  system and other well-known correlated superconductors, implying weaker electronic correlation.

## II. EXPERIMENT

$K_{0.65(3)}Fe_{1.41(4)}Se_{2.00(4)}$  (K-122) single crystals were synthesized by the self-flux method as described elsewhere in detail.<sup>38</sup> Thermal and electrical transport measurements were conducted in a Quantum Design PPMS-9 physical properties measurement system. The sample was cleaved to a rectangular shape with dimension  $5 \times 2$  mm<sup>2</sup> in the  $ab$  plane and  $0.3$   $\mu$ m thickness along the  $c$  axis. Thermoelectric power and thermal conductivity were measured using the steady state method and a one-heater-two-thermometer setup with silver paint contact directly on the sample surface. The heat and electrical current were transported within the  $ab$  plane of the crystal oriented by a Laue camera, with magnetic field along the  $c$  axis and perpendicular to the heat/electrical current. The sample is very sensitive to oxygen in air, and air exposure exceeding 1 h will result in significant surface oxidation seen by an incomplete transition in  $\rho(T)$  and  $\rho > 0$  below  $T_c$ . The exposure to air of samples we measured was less than 20 min. The clear and complete superconducting transition seen in  $\rho(T)$  and  $S(T)$  confirmed that the surface of our samples was not oxidized. The relative error in our measurement for both  $\kappa$  and  $S$  was below 5% based on a Ni standard measured under identical conditions.

## III. RESULTS AND DISCUSSION

The temperature dependence of the electrical resistivity  $\rho(T)$ , thermal conductivity  $\kappa(T)$ , and TEP  $S(T)$  for K-122 in zero magnetic field between 2 and 130 K is shown in Fig. 1.

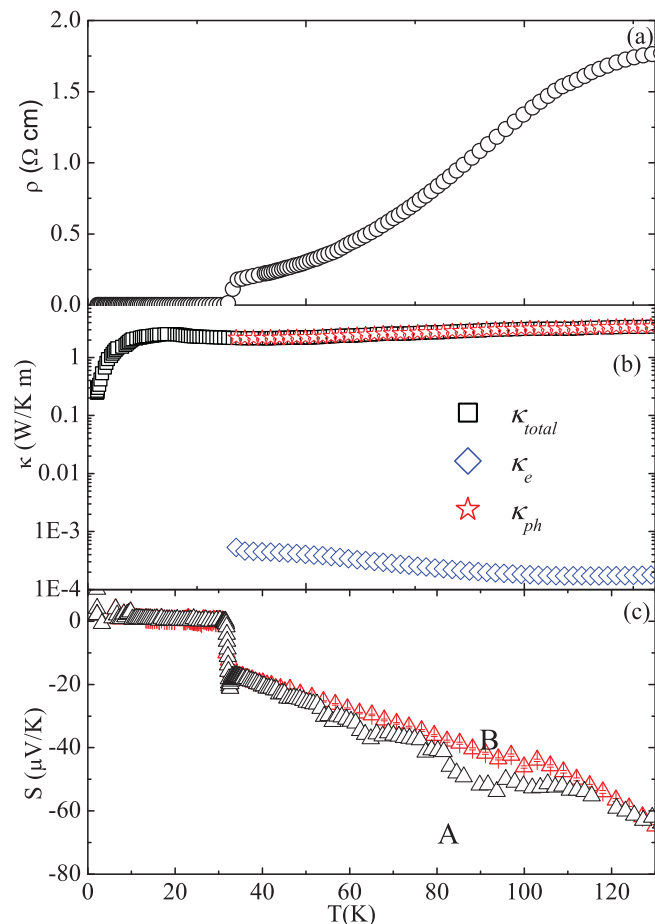


FIG. 1. (Color online) Temperature dependence of the resistivity (a), thermal conductivity (b), and thermoelectric power (c) for K-122 under zero magnetic field within a temperature range from 2 to 130 K. The electron term  $\kappa_e$  is estimated using the Wiedemann-Franz law and the phonon term  $\kappa_{ph}$  is obtained by subtracting the electron term from the total thermal conductivity (see text). We show the thermoelectric power  $S(T)$  for two independently grown samples A and B.

The  $\rho(T)$  is metallic below  $\sim 125$  K, and superconducting below  $\sim 32$  K. These values are similar to those in previous reports.<sup>23,24</sup> The thermal conductivity decreases with decrease in temperature in general, showing a peak below  $T_c$ . The thermoelectric power is negative, consistent with negative charge carriers. The TEP results for two independently grown samples are nearly identical. The value of the TEP decreases with decrease of temperature and exhibits nearly linear behavior up to 130 K. It vanishes at  $T_c$  since Cooper pairs carry no entropy. The  $T_c$  inferred from  $S(T) = 0$  for two samples is identical and is 31.8 K, consistent with resistivity measurement.

Figure 2(a) shows the thermal conductivity  $\kappa$  and electrical resistivity  $\rho$  near  $T_c$ . Below  $T_c$   $\kappa$  increases with decrease in temperature and peaks near  $\frac{T_c}{2}$  ( $\sim 17$  K). The peak in thermal conductivity below  $T_c$  was observed in hole-doped  $\text{Ba}_{1-x}\text{K}_x\text{Fe}_2\text{As}_2$ ,<sup>39</sup> electron-doped  $\text{Ba}(\text{Fe}_{1-x}\text{Co}_x)_2\text{As}_2$ ,<sup>40</sup> and other unconventional superconductors such as  $\text{YBa}_2\text{Cu}_3\text{O}_{7-\delta}$  (Ref. 41) and  $\text{CeCoIn}_5$ ,<sup>42</sup> where it was attributed to a large quasiparticle (QP) population and enhanced zero-field QP mean free path in the superconducting state. However, the resistivity in our sample is very high. Thermal conductivity

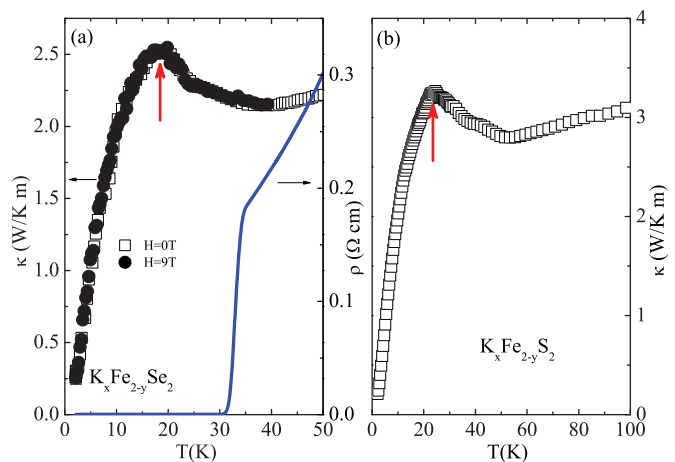


FIG. 2. (Color online) (a) Thermal conductivity in 0 (open squares) and 9 T (open circles) field, as well as electrical resistivity in 0 T field (red line) of K-122 near  $T_c$ . (b) Thermal conductivity in zero magnetic field for  $\text{K}_x\text{Fe}_{2-y}\text{S}_2$ . Red arrows indicate the position of the peak in thermal conductivity.

is composed of an electron term  $\kappa_e$  and a phonon term  $\kappa_{ph}$ ;  $\kappa_{total} = \kappa_e + \kappa_{ph}$ . The electron term  $\kappa_e$  above  $T_c$ , estimated using the Wiedemann-Franz law  $\frac{\kappa_e}{T} = \frac{L_0}{\rho}$ , is very small and indicates a predominantly phonon contribution [Fig. 1(b)]. In order to clarify the origin of this peak, we show [Fig. 2(b)] the thermal conductivity of  $\text{K}_x\text{Fe}_{2-y}\text{S}_2$ , which is a semiconductor with identical crystal structure and somewhat reduced lattice parameters.<sup>43</sup>  $\text{K}_x\text{Fe}_{2-y}\text{S}_2$  also exhibits a peak in thermal conductivity at  $\sim 22$  K that is obviously unrelated to  $T_c$ . Moreover, a 9 T magnetic field suppresses superconductivity in K-122 to 27 K.<sup>38,44</sup> This should suppress the peak in thermal conductivity induced by QPs, as seen in cuprates and  $\text{Ba}_{1-x}\text{K}_x\text{Fe}_2\text{As}_2$ .<sup>40,41</sup> However, a 9 T magnetic field has no significant influence on the peak observed in our sample, as shown by the open circles in Fig. 2(a). The peak in  $\kappa$  therefore is more likely to originate from phonons rather than the QP contribution. The phonon peak in lattice thermal conductivity is commonly found in materials due to the competition between the point-defect/boundary scattering and the umklapp phonon scattering mechanism.<sup>45</sup>

Figure 3 presents  $\rho(T)$  and  $S(T)$  near  $T_c$  in different magnetic fields up to 9 T. The resistive transition strongly broadens, and both the onset temperature and the zero resistance are suppressed. The superconducting transition seen by TEP is also suppressed and broadened by an external field but the amplitude of the normal state Seebeck response does not change for  $\mu_0 H < 9$  T. These features are reminiscent of the thermally induced motion of vortex lattices in superconductors. A small peak just above  $T_c$  in the TEP is observed only under zero field, as shown by the red arrow in Fig. 3(b). This is similar to some TEP observed in cuprates and is attributed to the ac measuring technique.<sup>46,47</sup> The ac measurement technique picks up a voltage contribution of the thermoelectric power derivative in addition to the linear term. This is present even for good thermal contacts and is reduced for a lower density of data points and sharp transitions.

In the lower part of the transition ( $\frac{\rho}{\rho_n} \leq 1\%$ ),  $\rho(T)$  is thermally activated according to the Arrhenius law

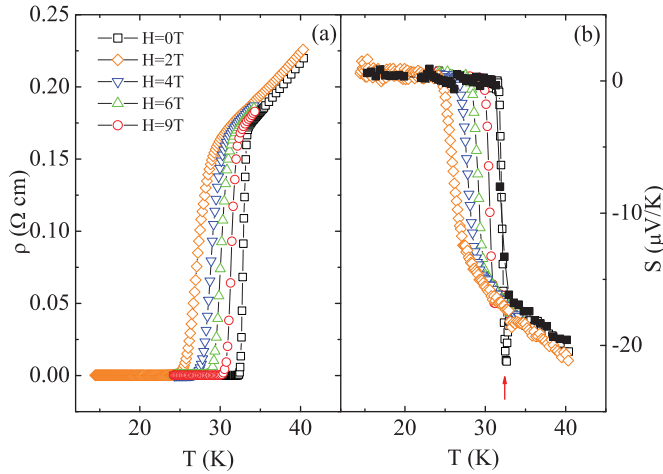


FIG. 3. (Color online) Temperature dependence of resistivity (a) and Seebeck coefficient (b) of K-122 in different magnetic fields in the temperature range between 2 and 40 K. For TEP, zero-field data of sample B (closed squares) are shown for comparison. The red arrow indicates the small peak position just above  $T_c$  in the TEP.

$\rho = \rho_0 \exp(-\frac{U_a(B)}{k_B T})$ , where  $U_a(B)$  is the activation energy for the flux motion. A linear behavior occurs over a typical temperature interval of about 6 K. The Seebeck coefficient follows identical temperature dependence in the same region. Figures 4(a) and 4(b) show the Arrhenius plots of  $\ln(\rho)$  and  $\ln(S)$  as a function of the inverse temperature. The conventional theory cannot reproduce the large TEP in the mixed state, similarly to the high- $T_c$  cuprates.<sup>48,49</sup> The activation energy for the flux motion obtained from resistivity decreases exponentially with magnetic field, but the value obtained from the TEP is nearly unchanged and larger, as shown in Fig. 4(c), also in contrast to the conventional theory of flux motion.

TEP is associated with entropy and heat transport parallel to the “induced” electric field. This longitudinal entropy flow is not carried by the normal excitations in the vortex cores since these excitations move with the vortices perpendicular to the induced electric field (Nernst effect).<sup>49</sup> The longitudinal entropy transport has to be attributed to other excitations. We postulate that TEP in the mixed state near  $T_c$  is attributable to quasi-particles excited over the energy gap as in high- $T_c$  cuprates.<sup>48,49</sup> Such excitations, not bound to the vortex core, are present in any superconductor at finite temperature and may be important in determining the dissipation due to the short coherence length.<sup>48,49</sup> Therefore, an estimate of the TEP can be obtained from

$$\frac{S_M}{S_N} \simeq \frac{\rho_M}{\rho_N}, \quad (1)$$

where  $S_M, \rho_M, S_N, \rho_N$  are the TEP and resistivity in the mixed ( $M$ ) and normal states ( $N$ ), respectively, since the TEP from longitudinal entropy flow has a small dependence on the Hall angle.<sup>49</sup> This is in a good agreement with experimental data, as shown in Fig. 4(d).

We now turn to the TEP in the normal state. TEP is the sum of three different contributions: the diffusion term  $S_{\text{diff}}$ , the spin-dependent scattering term, and the phonon-drag term  $S_{\text{drag}}$  due to electron-phonon coupling.<sup>32,50</sup> The spin-dependent scattering or corresponding magnon drag effect always gives

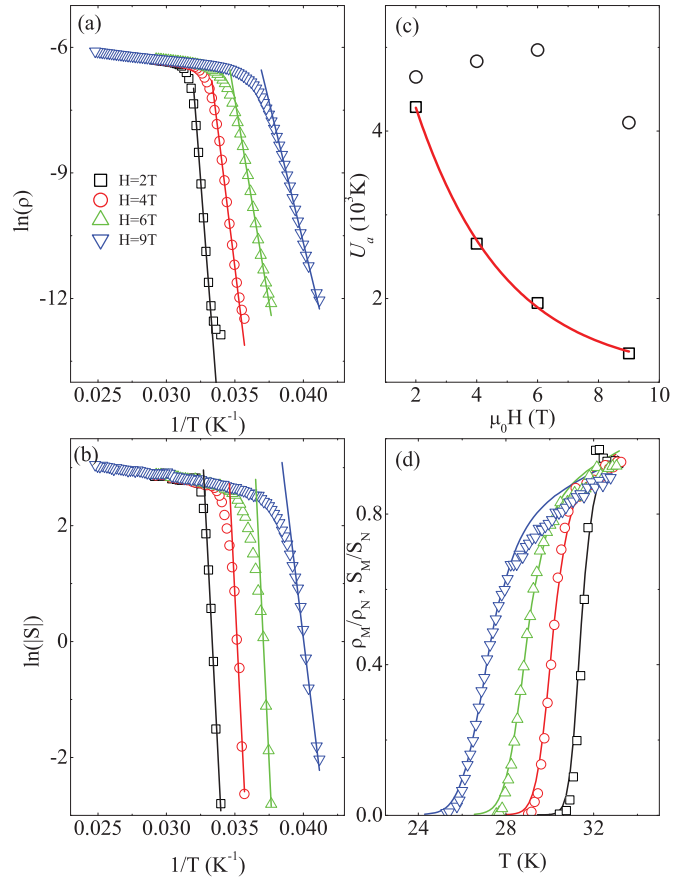


FIG. 4. (Color online) Arrhenius plots of resistivity (a) and Seebeck coefficient (b). (c) The activation energy for flux motion derived from resistivity data (open squares) and TEP data (open circles) under different magnetic fields. The red line is the exponential fitting results for the data from resistivity. (d) The relationship between  $S_M/S_N$  (open symbols),  $\rho_M/\rho_N$  (solid lines), and temperature under different magnetic fields.

$\sim T^{3/2}$  dependence,<sup>51</sup> which is not observed in our TEP results. Moreover, TEP in our sample above  $T_c$  is independent of magnetic field, which excludes the spin-dependent mechanism. The contribution of the phonon-drag term often gives  $\sim T^3$  dependence for  $T \ll \Theta_D$ ,  $\sim 1/T$  for  $T \geq \Theta_D$  (where  $\Theta_D$  is the Debye temperature), and a peak structure for  $\sim \frac{\Theta_D}{5}$ .<sup>52,53</sup> The estimated Debye temperature of the K-122 system is about 260 K.<sup>54</sup> The absence of the peak structure in our TEP results suggests a negligible contribution of the phonon-drag effect to  $S(T)$ . Instead a nearly linear relationship is observed between 2 and 120 K [Fig. 1(c)], suggesting that the diffusion term is dominant.

The diffusive Seebeck response of a Fermi liquid is expected to be linear in  $T$  in the zero-temperature limit, with a magnitude proportional to the strength of electronic correlations.<sup>55</sup> This is similar to the  $T$ -linear electronic specific heat,  $C_e/T = \gamma$ . Both can be linked to the Fermi temperature  $T_F$ :

$$S/T = \pm \frac{\pi^2 k_B}{2} \frac{1}{e T_F}, \quad (2)$$

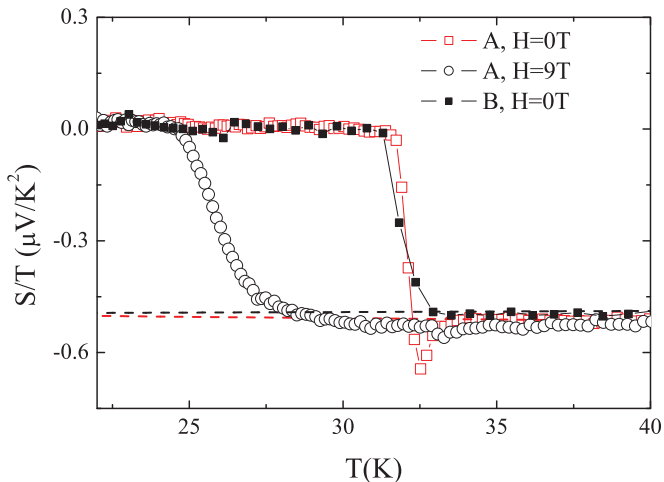


FIG. 5. (Color online) Temperature dependence of the Seebeck coefficient divided by  $T$ ,  $S/T$ , in  $K_{0.8}Fe_{2-y}Se_2$  under 0 (open squares) and 9 T (open circles) magnetic field for sample A, and under 0 T (closed squares) for sample B. The dashed lines are the linear fitting result within the higher temperature range.

$$\gamma = \frac{\pi^2}{2} k_B \frac{n}{T_F}, \quad (3)$$

where  $k_B$  is Boltzmann's constant,  $e$  is the electron charge, and  $n$  is the carrier density.<sup>34</sup> Figure 5 presents the temperature dependence of the TEP divided by  $T$ ,  $S/T$ , under 0 (open squares) and 9 T (open circles) magnetic field for sample A and 0 T (closed squares) for sample B. TEP in the normal state near  $T_c$  is independent of magnetic field and can be described well by the diffusive model. The zero-temperature extrapolated value of  $S/T$  is  $\sim 0.48 \mu\text{V}/\text{K}$  for  $\mu_0 H < 9 \text{ T}$  (Fig. 5). We can therefore extract  $T_F = 880 \text{ K}$ .

The ratio of the superconducting transition temperature to the normalized Fermi temperature,  $\frac{T_c}{T_F}$ , characterizes the correlation strength in superconductors. In unconventional superconductors, such as  $CeCoIn_5$  (Ref. 56) and  $YBa_2Cu_3O_{6.67}$ ,<sup>57</sup> this ratio is about 0.1, but it is only  $\sim 0.02$  in BCS superconductors, such as  $LuNi_2B_2C$ .<sup>34</sup> In  $Fe_{1+y}Te_{1-x}Se_x$ ,  $\frac{T_c}{T_F}$  is also near 0.1, pointing to the importance of electronic correlations.<sup>34</sup> When compared to these strongly correlated superconductors,  $\frac{T_c}{T_F} \sim 0.04$  in our crystal is relatively small, but is larger than in conventional superconductors. This implies that K-122 is a weakly or intermediately correlated superconductor. K-122 is proposed to be an iron-based high-temperature superconductor near insulating antiferromagnetic order, just like cuprates, whose parent compound is a Mott insulator and where the correlation effects dominate.<sup>25</sup> However, a transmission electron microscope study demonstrated the presence of ordered Fe vacancies in the  $ab$  plane<sup>58</sup> and a theoretical study pointed out that the ordered Fe vacancies could induce band narrowing and consequently decrease the correlation strength needed for the Mott transition.<sup>59</sup> This could explain the relatively weak correlation strength observed in our experiment.

Recent specific heat measurement<sup>54</sup> find  $\gamma_n = 6 \pm 0.5 \text{ mJ}/\text{mol K}^2$ , which is smaller than in iron-based superconductors. The absolute value of the dimensionless ratio of TEP

TABLE I. Set of derived parameters for  $K_{0.8}Fe_{2-y}Se_2$ .

Quantity	Magnitude
$k_F$ ( $\text{nm}^{-1}$ )	2.6
$\xi$ (nm)	1.8
$m^*$ (units of $m_e$ )	3.4
$v_F$ (km/s)	89

to specific heat,  $q = \frac{N_{Av}eS}{T\gamma}$ , with  $N_{Av}$  the Avogadro number, provides the carrier density.<sup>55</sup> Calculation gives the carrier density with  $|q|^{-1} \simeq 0.13$  carriers per unit cell, which is somewhat larger than the value in  $Fe_{1+y}Te_{0.6}Se_{0.4}$ .<sup>34</sup> Given the volume of the unit cell, we obtain the carrier density per volume  $n \simeq 6.1 \times 10^{20} \text{ cm}^{-3}$  and derive the Fermi momentum  $k_F = (3\pi^2 n)^{1/3} \simeq 2.6 \text{ nm}^{-1}$ . Ultimately we can derive the effective mass  $m^*$ , Fermi velocity  $v_F$ , and the superconducting coherence length  $\xi$  using  $k_B T_F = \frac{\hbar^2 k_F^2}{2m^*}$ ,  $\hbar k_F = m^* v_F$ , and  $\xi = \frac{\hbar v_F}{\pi \Delta_0}$  with  $\Delta_0 = 10.3 \text{ meV}$  measured by angle-resolved photoemission spectroscopy.<sup>28</sup> The results are listed in Table I. It is worth noting that  $\xi$  can also be derived from the upper critical field  $H_{c2}$ , using  $H_{c2}(0) = 0.693[-\frac{dH_{c2}}{dT}]_{T_c} T_c$  and  $\xi^{-2} = \frac{2\pi}{\Phi_0} \frac{H_{c2}(0)}{T_c}$ . From Ref. 24,  $[-\frac{dH_{c2}}{dT}]_{T_c} = 3.17 \text{ T/K}$ , and the derived superconducting coherence length is  $\xi \simeq 2.2 \text{ nm}$ , consistent with value in Table I. This confirms the consistency of our derived parameters.

#### IV. CONCLUSION

Thermal transport measurement of the iron-based superconductor  $K_xFe_{2-y}Se_2$  have been performed on a single-crystalline sample. The peak anomaly in thermal conductivity observed at nearly  $\frac{T_c}{2} \sim 17 \text{ K}$  is attributed to the phonon contribution. The large thermoelectric power in the mixed state could imply large quasiparticle excitations over the energy gap. The thermoelectric power above  $T_c$  exhibits nearly linear behavior and could be described well by the carrier diffusion mechanism in a wide temperature range. The zero-temperature extrapolated thermoelectric power is smaller when compared to other correlated superconductors, pointing to a large normalized Fermi temperature. These findings indicate that  $K_xFe_{2-y}Se_2$  is a weakly or intermediately correlated superconductor. The ordered Fe vacancies could induce band narrowing and then decrease the correlation strength needed for the Mott transition, as predicted by theory.

*Note added.* We recently became aware of Ref. 60 with similar thermopower data in zero field.

#### ACKNOWLEDGMENTS

We acknowledge valuable discussions with Louis Taillefer. We thank John Warren for help with scanning electron microscope measurements. Work at Brookhaven is supported by the US DOE under Contract No. DE-AC02-98CH10886 and in part by the center for Emergent Superconductivity, and Energy Frontier Research Center funded by the US DOE, office for Basic Energy Science.

- <sup>1</sup>Y. Kamihara, T. Watanabe, M. Hirano, and H. Hosono, *J. Am. Chem. Soc.* **130**, 3296 (2008).
- <sup>2</sup>I. I. Mazin, *Nature (London)* **464**, 183 (2010).
- <sup>3</sup>D. C. Johnson, *Adv. Phys.* **59**, 803 (2010).
- <sup>4</sup>G. F. Chen, Z. Li, D. Wu, G. Li, W. Z. Hu, J. Dong, P. Zheng, J. L. Luo, and N. L. Wang, *Phys. Rev. Lett.* **100**, 247002 (2008).
- <sup>5</sup>Z.-A. Ren, J. Yang, W. Lu, W. Yi, H.-C. Che, X.-L. Dong, L.-L. Sun, F. Zhou, and Z.-X. Zhao, *Mater. Res. Innovations* **12**, 1 (2008).
- <sup>6</sup>X. H. Chen, T. Wu, G. Wu, R. H. Liu, H. Chen, and D. F. Fang, *Nature (London)* **453**, 761 (2008).
- <sup>7</sup>Z.-A. Ren, W. Lu, W. Yi, H.-C. Che, X.-L. Shen, Z.-C. Li, G.-C. Chen, X.-L. Dong, L.-L. Sun, F. Zhou, and Z.-X. Zhao, *Chin. Phys. Lett.* **25**, 2215 (2008).
- <sup>8</sup>C. Wang, L. Li, S. Chi, Z. Zhu, Z. Ren, Y. Li, Y. Wang, X. Lin, Y. Luo, S. Jiang, X. Xu, G. Cao, and Z. Xu, *Europhys. Lett.* **83**, 67006 (2008).
- <sup>9</sup>A. Leithe-Jasper, W. Schnelle, C. Geibel, and H. Rosner, *Phys. Rev. Lett.* **101**, 207004 (2008).
- <sup>10</sup>M. Rotter, M. Tegel, and D. Johrendt, *Phys. Rev. Lett.* **101**, 107006 (2008).
- <sup>11</sup>G. Mu, H. Luo, Z. Wang, L. Shan, C. Ren, and H.-H. Wen, *Phys. Rev. B* **79**, 174501 (2009).
- <sup>12</sup>X. C. Wang, Q. Q. Liu, Y. X. Lv, W. B. Gao, L. X. Yang, R. C. Yu, F. Y. Li, and C. Q. Jin, *Solid State Commun.* **148**, 538 (2008).
- <sup>13</sup>J. H. Tapp, Z. Tang, B. Lv, K. Sasmal, B. Lorenz, Paul C. W. Chu, and A. M. Guloy, *Phys. Rev. B* **78**, 060505 (2008).
- <sup>14</sup>F. C. Hsu, J. Y. Luo, K. W. Yeh, T. K. Chen, T. W. Huang, P. M. Wu, Y. C. Lee, Y. L. Huang, Y. Y. Chu, C. L. Chen, J. Y. Luo, D. C. Yan, and M. K. Wu, *Proc. Natl. Acad. Sci. USA* **105**, 14262 (2008).
- <sup>15</sup>Y. Mizuguchi, F. Tomooka, S. Tsuda, T. Yamaguchi, and Y. Takano, *Appl. Phys. Lett.* **94**, 012503 (2009).
- <sup>16</sup>I. I. Mazin, D. J. Singh, M. D. Johannes, and M. H. Du, *Phys. Rev. Lett.* **101**, 057003 (2008).
- <sup>17</sup>K. Kuroki, S. Onari, R. Arita, H. Usui, Y. Tanaka, H. Kontani, and H. Aoki, *Phys. Rev. Lett.* **101**, 087004 (2008).
- <sup>18</sup>X. F. Wang, T. Wu, G. Wu, H. Chen, Y. L. Xie, J. J. Ying, Y. J. Yan, R. H. Liu, and X. H. Chen, *Phys. Rev. Lett.* **102**, 117005 (2009).
- <sup>19</sup>J. K. Dong, S. Y. Zhou, T. Y. Guan, H. Zhang, Y. F. Dai, X. Qiu, X. F. Wang, Y. He, X. H. Chen, and S. Y. Li, *Phys. Rev. Lett.* **104**, 087005 (2010).
- <sup>20</sup>K. Terashima, Y. Sekiba, J. H. Bowen, K. Nakayama, T. Kawahara, T. Sato, P. Richard, Y.-M. Xu, L. J. Li, G. H. Cao, Z.-A. Xu, H. Ding, and T. Takahashi, *Proc. Natl. Acad. Sci. USA* **106**, 7330 (2009).
- <sup>21</sup>Y. Xia, D. Qian, L. Wray, D. Hsieh, G. F. Chen, J. L. Luo, N. L. Wang, and M. Z. Hasan, *Phys. Rev. Lett.* **103**, 037002 (2009).
- <sup>22</sup>A. V. Balatsky and D. Parker, *Physics* **2**, 59 (2009).
- <sup>23</sup>J. G. Guo, S. F. Jin, G. Wang, S. C. Wang, K. X. Zhu, T. T. Zhou, M. He, and X. L. Chen, *Phys. Rev. B* **82**, 180520 (2010).
- <sup>24</sup>J. J. Ying, X. F. Wang, X. G. Luo, A. F. Wang, M. Zhang, Y. J. Yan, Z. J. Xiang, R. H. Liu, P. Cheng, G. J. Ye, and X. H. Chen, *New J. Phys.* **13**, 033008 (2011).
- <sup>25</sup>M. H. Fang, H. D. Wang, C. H. Dong, Z. J. Li, C. M. Feng, J. Chen, and H. Q. Yuan, *Euro. Phys. Lett.* **94**, 27009 (2011).
- <sup>26</sup>C. H. Li, B. Shen, F. Han, X. Y. Zhu, and H. H. Wen, e-print [arXiv:1012.5637](https://arxiv.org/abs/1012.5637).
- <sup>27</sup>A. F. Wang, J. J. Ying, Y. J. Yan, R. H. Liu, X. G. Guo, Z. Y. Li, X. F. Wang, M. Zhang, G. J. Ye, P. Cheng, Z. J. Xiang, and X. H. Chen, *Phys. Rev. B* **83**, 060512 (2011).
- <sup>28</sup>Y. Zhang, L. X. Yang, M. Xu, Z. R. Ye, F. Chen, C. He, J. Jiang, B. P. Xie, J. J. Ying, X. F. Wang, X. H. Chen, J. P. Hu, and D. L. Feng, *Nature Mater.* **10**, 273 (2011).
- <sup>29</sup>X.-P. Wang, T. Qian, P. Richard, P. Zhang, J. Dong, H.-D. Wang, C.-H. Dong, M.-H. Fang, and H. Ding, *Europhys. Lett.* **93**, 57001 (2011).
- <sup>30</sup>Daixiang Mou, Shanyu Liu, Xiaowen Jia, Junfeng He, Yingying Peng, Li Yu, Xu Liu, Guodong Liu, Shaolong He, Xiaoli Dong, Jun Zhang, J. B. He, D. M. Wang, G. F. Chen, J. G. Guo, X. L. Chen, Xiaoyang Wang, Qinjun Peng, Zhimin Wang, Shenjin Zhang, Feng Yang, Zuyan Xu, Chuangtian Chen, and X. J. Zhou, *Phys. Rev. Lett.* **106**, 107001 (2011).
- <sup>31</sup>A. S. Sefat, M. A. McGuire, B. C. Sales, R. Jin, J. Y. Howe, and D. Mandrus, *Phys. Rev. B* **77**, 174503 (2008).
- <sup>32</sup>N. Kang, P. Auban-Senzier, C. R. Pasquier, Z. A. Ren, J. Yang, G. C. Chen, and Z. X. Zhao, *New J. Phys.* **11**, 025006 (2009).
- <sup>33</sup>E. D. Mun, S. L. Bud'ko, Ni Ni, A. N. Thaler, and P. C. Canfield, *Phys. Rev. B* **80**, 054517 (2009).
- <sup>34</sup>A. Pourret, L. Malone, A. B. Antunes, C. S. Yadav, P. L. Paulose, B. Fauque, and K. Behnia, *Phys. Rev. B* **83**, 020504 (2011).
- <sup>35</sup>M. Matusiak, T. Plackowski, Z. Bukowski, N. D. Zhigadlo, and J. Karpinski, *Phys. Rev. B* **79**, 212502 (2009).
- <sup>36</sup>N. P. Butch, S. R. Saha, X. H. Zhang, K. Kirshenbaum, R. L. Greene, and J. Paglione, *Phys. Rev. B* **81**, 024518 (2010).
- <sup>37</sup>M. A. Tanatar, J.-Ph. Reid, H. Shakeripour, X. G. Luo, N. Doiron-Leyraud, N. Ni, S. L. Bud'ko, P. C. Canfield, R. Prozorov, and Louis Taillefer, *Phys. Rev. Lett.* **104**, 067002 (2010).
- <sup>38</sup>H. Lei, and C. Petrovic, e-print [arXiv:1102.1010](https://arxiv.org/abs/1102.1010).
- <sup>39</sup>J. G. Checkelsky, L. Li, G. F. Chen, J. L. Luo, N. L. Wang, and N. P. Ong, e-print [arXiv:0811.4668](https://arxiv.org/abs/0811.4668).
- <sup>40</sup>Y. Machida, K. Tomokuni, T. Isono, K. Izawa, Y. Nakajima, and T. Tamegai, *J. Phys. Soc. Jpn.* **78**, 073705 (2009).
- <sup>41</sup>Y. Zhang, N. P. Ong, P. W. Anderson, D. A. Bonn, R. Liang, and W. N. Hardy, *Phys. Rev. Lett.* **86**, 890 (2001).
- <sup>42</sup>K. Krishana, N. P. Ong, Y. Zhang, Z. A. Xu, R. Gagnon, and L. Taillefer, *Phys. Rev. Lett.* **82**, 5108 (1999).
- <sup>43</sup>H. Lei and C. Petrovic, e-print [arXiv:1101.5616](https://arxiv.org/abs/1101.5616).
- <sup>44</sup>Y. Mizuguchi, H. Takeya, Y. Kawasaki, T. Ozaki, S. Tsuda, T. Yamaguchi, and Y. Takano, *Appl. Phys. Lett.* **98**, 042511 (2011).
- <sup>45</sup>J. Yang, in *Thermal Conductivity: Theory, Properties and Applications*, edited by T. M. Tritt, (Kluwer Academic, New York, 2004).
- <sup>46</sup>M. Putti, M. R. Cimberle, A. Canesi, C. Foglia, and A. S. Siri, *Phys. Rev. B* **58**, 12344 (1998).
- <sup>47</sup>O. Maldonado, *Cryogenics* **32**, 908 (1992).
- <sup>48</sup>A. Dascoulidou, M. Galfy, C. Hohn, N. Knauf, and A. Freimuth, *Physica C* **201**, 202 (1992).
- <sup>49</sup>R. P. Huebener, *Supercond. Sci. Technol.* **8**, 189 (1995).
- <sup>50</sup>C. M. Bhandari, in *CRC Handbook of Thermoelectrics*, edited by D. M. Roew (CRC Press, Boca Raton, FL, 1995).
- <sup>51</sup>F. J. Blatt, D. J. Flood, V. Rowe, P. A. Schroeder, and J. E. Cox, *Phys. Rev. Lett.* **18**, 395 (1967).
- <sup>52</sup>R. D. Barnard, *Thermoelectricity in Metals and Alloys* (Taylor & Francis, London, 1972).
- <sup>53</sup>J. L. Cohn, S. A. Wolf, V. Selvamanickam, and K. Salama, *Phys. Rev. Lett.* **66**, 1098 (1991).

- <sup>54</sup>Bin Zeng, Bing Shen, Genfu Chen, Jianbao He, Duming Wang, Chunhong Li, and Hai-Hu Wen, *Phys. Rev. B* **83**, 144511 (2011).
- <sup>55</sup>K. Behnia, D. Jaccard, and J. Flouquet, *J. Phys.: Condens. Matter* **16**, 5187 (2004).
- <sup>56</sup>K. Izawa *et al.*, *Phys. Rev. Lett.* **99**, 147005 (2007).
- <sup>57</sup>J. Chang *et al.*, *Phys. Rev. Lett.* **104**, 057005 (2010).
- <sup>58</sup>Z. Wang, Y. J. Song, H. L. Shi, Z. W. Wang, Z. Chen, H. F. Tian, G. F. Chen, J. G. Guo, H. X. Yang, and J. Q. Li, *Phys. Rev. B* **83**, 140505 (2011).
- <sup>59</sup>R. Yu, J.-X. Zhu, and Q. Si, e-print [arXiv:1101.3307](https://arxiv.org/abs/1101.3307).
- <sup>60</sup>R. Hu, K. Cho, H. Kim, H. Hodovanets, W. E. Straszheim, M. A. Tanatar, R. Prozorov, S. L. Bud'ko, and P. C. Canfield, *Supercond. Sci. Technol.* **24**, 065006 (2011).